Capece et al., https://doi.org/10.1083/jcb.201609072

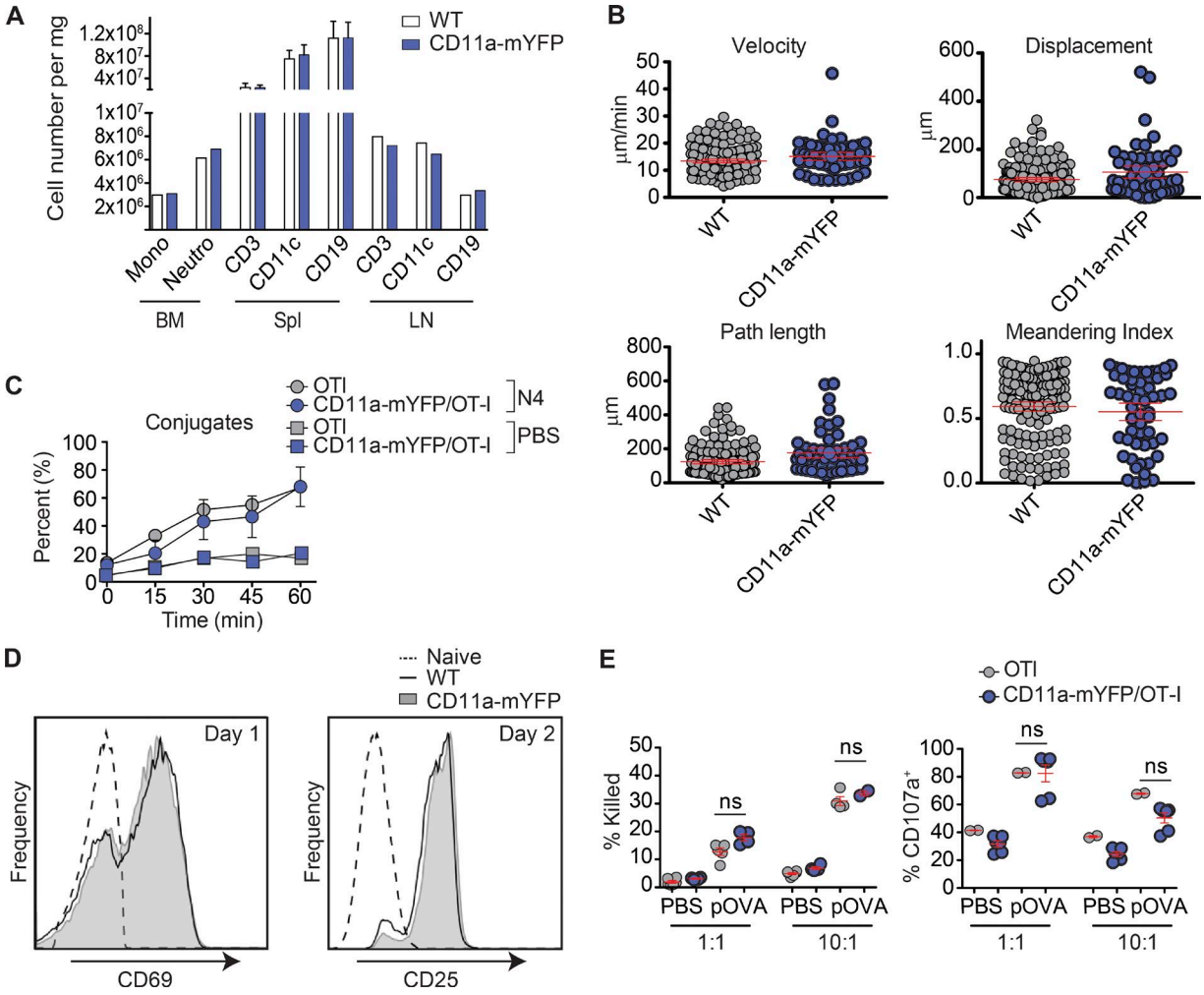

Figure S1. **CD11a-mYFP mice show normal LFA-1 expression and function.** (A) Number of cells from specified organs of WT and CD11a-mYFP$^{+/+}$ (Homo) mice; n = 4 mice. (B–D) Naive CD8^{+} T cells from CD11a-mYFP/OT-I and WT OT-I mice have comparable migration on ICAM-1+CCL21–coated plates (B; circles represent individual cells from four independent experiments with mean shown as a line) flow cytometry–based conjugation rates with antigen (Ag)-bearing BMDCs (C; n = 4–8 mice per group, PBS; percentage of conjugations with PBS-treated APCs), and surface levels of activation markers when activated with OVA-loaded irradiated splenocytes in vitro for indicated times (D; n = 3, 9 mice per group). (E) Activated CD8^{+} T cells kill antigen-bearing target cells (left) and degranulate (right) equally well at various ratios (n = 3 mice per group). Data are expressed as mean ± SEM.

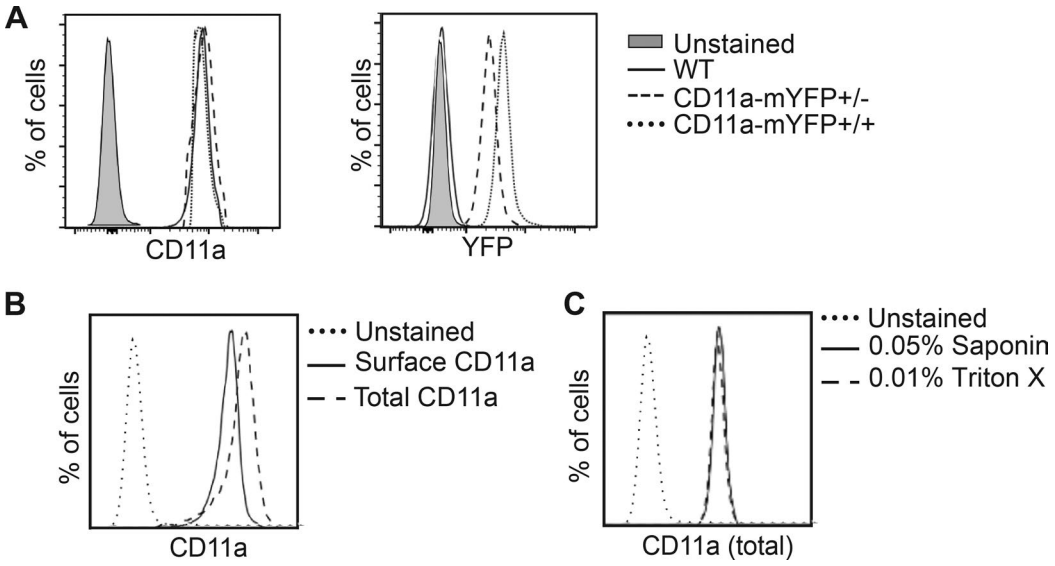

Figure S2. **WT and CD11a-mYFP naive CD8⁺ T cells express intracellular LFA-1.** (A) Representative flow cytometry of CD11a antibody (Ab) staining (left, surface LFA-1) and mYFP intensities (right, total LFA-1) from WT, CD11a-mYFP$^{+/}$ (Het), and CD11a-mYFP$^{+/+}$ (Homo) mice; *n* = 6 mice. (B) Representative flow cytometry of surface (nonpermeabilized) and total (permeabilized with saponin) CD11a antibody staining of WT CD8⁺ T cells; *n* = 6 mice. (C) Representative flow cytometry of intracellular CD11a antibody staining (total) of WT CD8⁺ T cells permeabilized with 0.05% saponin or 0.01% Triton X-100 for 15 min; *n* = 3 mice.

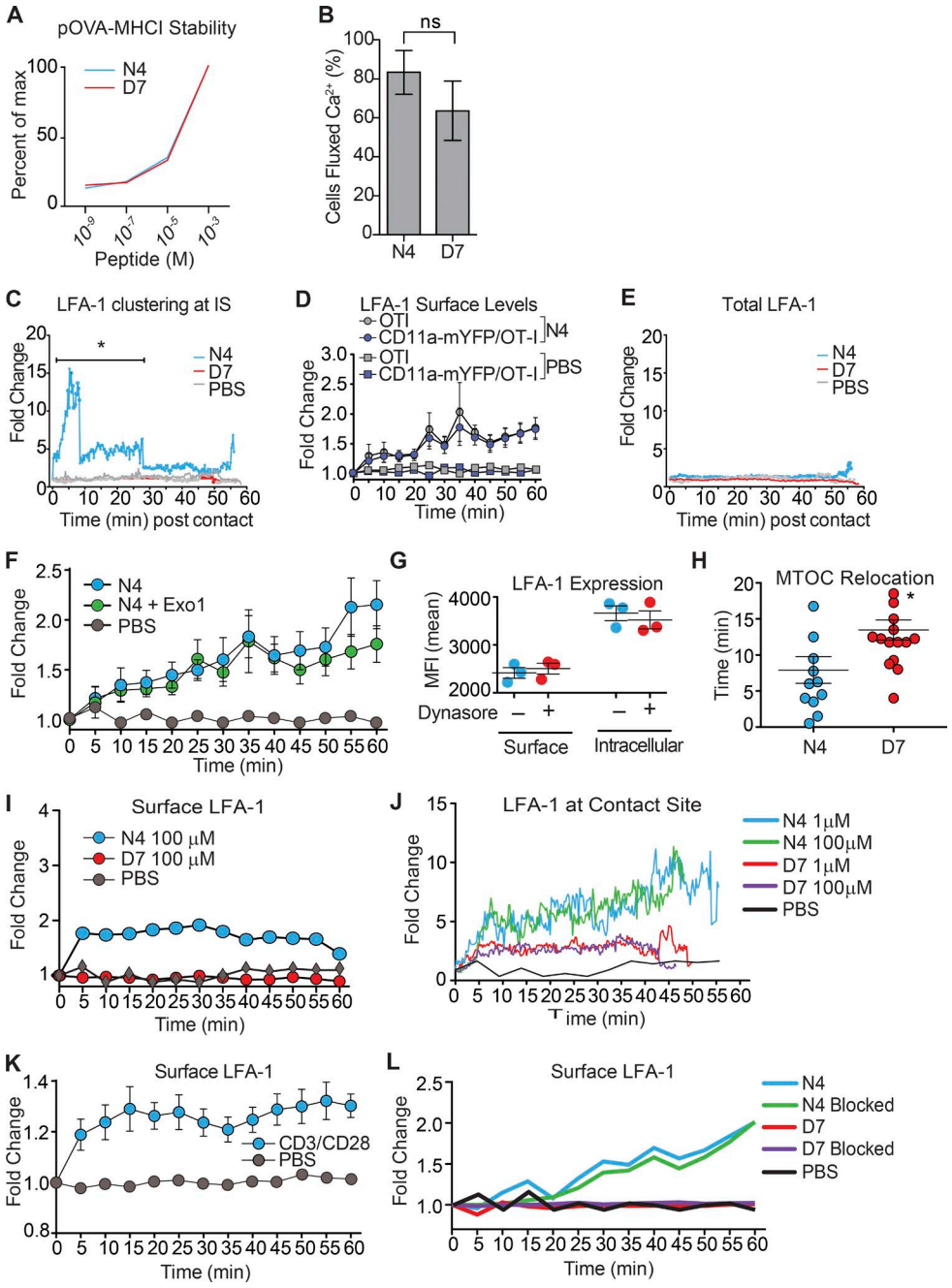

Figure S3. **LFA-1 redistribution to the cell surface.** (A) Flow cytometry analysis of peptide stability of cognate ligand N4 and APL D7 in MHC class I molecules on the surface of RMA-S cells. RMA-S cells were pulsed with various concentrations of peptide for 1 h, washed extensively, and incubated for 3 h at 37°C. MHC class I (H2Kb) antibody was used to detect surface peptide levels by flow cytometry. Data are expressed as mean of three independent experiments. (B) Calcium flux of calcium Crimson-AM–labeled naive CD8+ T cells after contact with antigen-bearing BMDCs was measured via microscopy. Data are expressed as mean ± SEM of three separate experiments (one mouse per experiment; 30–45 cells per mouse; ns, not significant). (C and E) Quantification of relative fluorescence intensity of CD11a-mYFP at the contact site (C) and for the total cell (E) from corresponding data in Fig. 2 (B and C). Data are expressed as mean of total 30–50 cells. *, $P < 0.05$. (D) Flow cytometry analysis of surface LFA-1 expression after indicated times of T cell and OVA-loaded or PBS-treated APC contacts with CD8+ T cells from WT OT-I and CD11a-mYFP/OT-I mice. Data are expressed as mean ± SEM of 9–12 experiments. (F) Flow cytometry analysis of cell surface LFA-1 expression levels after indicated times of T cell–APC contacts. T cells were pretreated for 10 min with 10 μm Exo1. Data are expressed as mean ± SEM of six to eight mice. (G) Surface and total (intracellular) LFA-1 levels as measured by anti–CD11a antibody staining of naive WT CD8+ T cells treated with 10 μM Dynasore for 15 min; $n = 3$ mice per group. (H) MTOC relocation time after contact with antigen (N4 or D7)–bearing BMDCs was measure by real-time microscopy (based on ER Tracker staining). Note that both N4 and D7 induced complete MTOC relocalization after contact with BMDCs; thus, TCR signaling was intact but D7 did not induce intracellular LFA-1 translocation. Circles represent individual cells from three independent experiments with mean shown as a line. Data represent mean ± SEM. *, $P < 0.05$. (I) Flow cytometry analysis of cell surface LFA-1 expression levels after indicated times of T cell–APC contacts at high antigen concentration. Data are expressed as mean of six mice. (J) Quantification of relative fluorescence intensity of CD11a-mYFP at the contact site with high concentration Ag-bearing BMDCs, Data are expressed as mean of 3 mice. (K) Flow cytometry analysis of cell surface LFA-1 expression levels after indicated times of contact with CD3/CD28 coated beads. Data are expressed as mean ± SEM of six mice. (L) Flow cytometry analysis of cell surface LFA-1 expression levels after indicated times of T cell–APC contacts. T cells were pretreated for 15 min with 100 μg CD11a blocking antibody (M17/4). Data are expressed as mean of six mice.

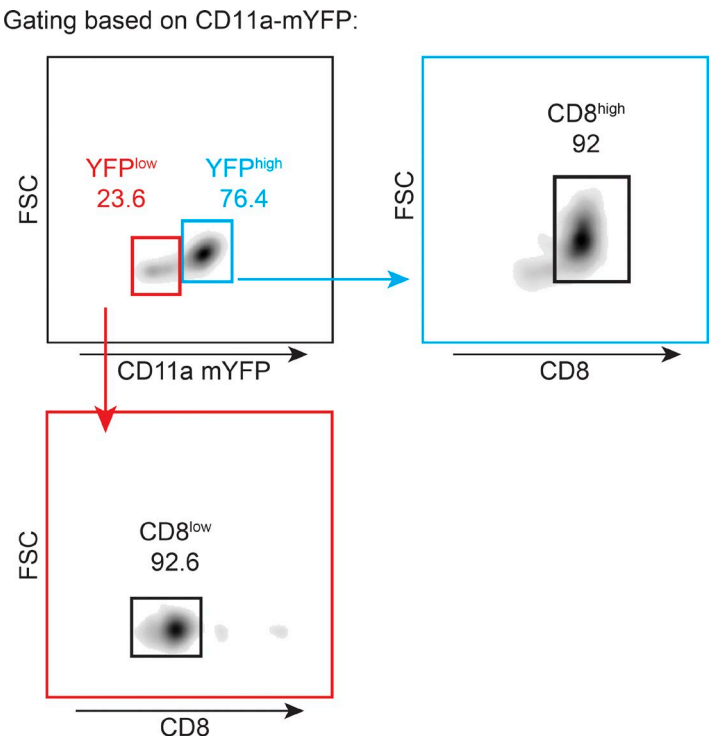

Figure S4. **Naive CD11a-mYFP/OT-I CD8+ T cells (1–3 × 10^6) were labeled with Cell Proliferation Dye eFluor670 and i.v. transferred 24 h before infection with influenza virus x31-OVA.** 56 h after infection, transferred cells were sorted, identified as the first division based on proliferation dye expression, stained with anti-CD8 antibody, and analyzed by flow cytometry for correlation of CD11a-mYFP high and low populations with CD8 expression (n = 3 mice).

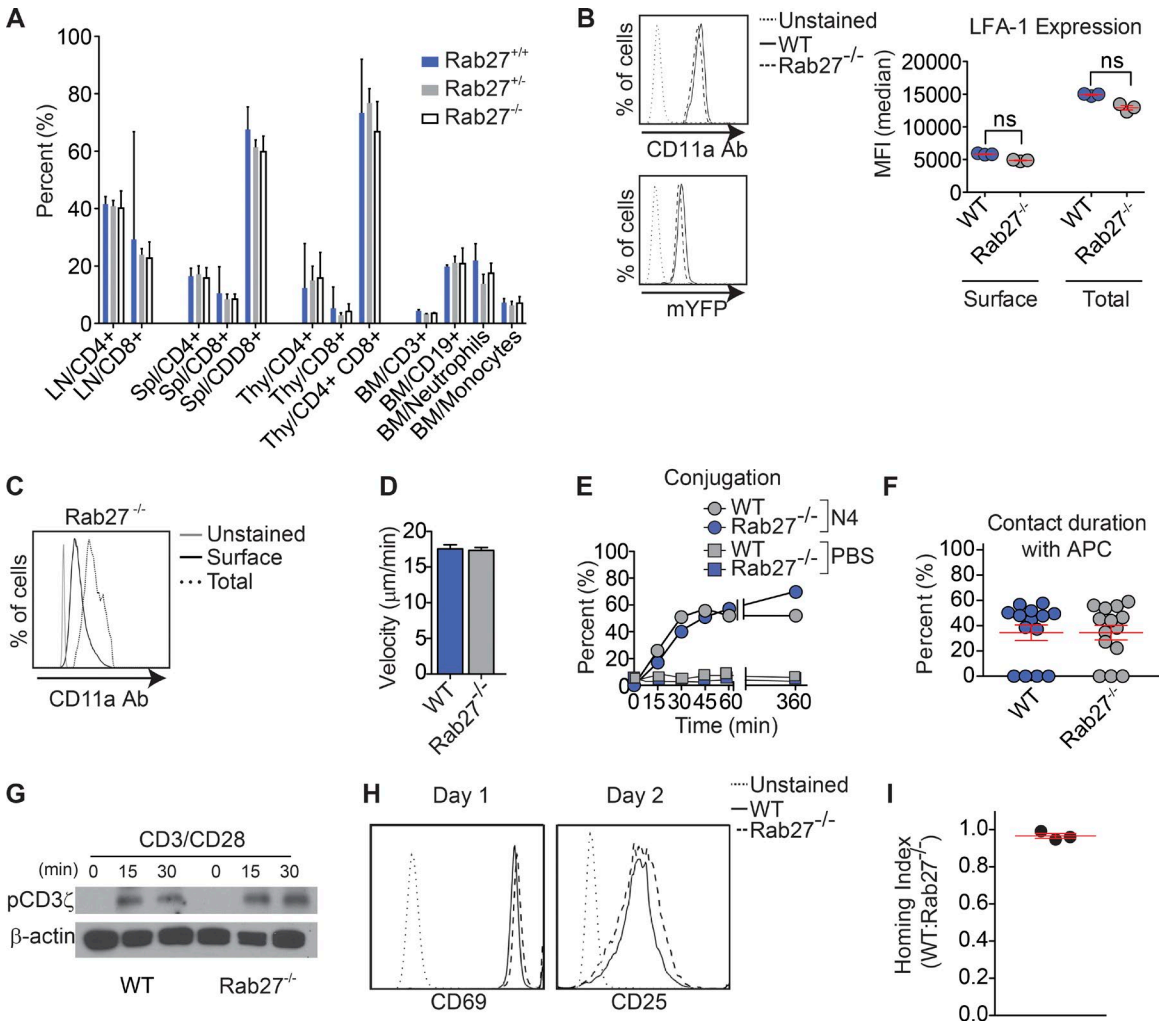

Figure S5. **LFA-1 expression and functions are comparable in naive CD8⁺ T cells from WT and Rab27 KO mice.** (A) Frequency of indicated cells from flow cytometry of specified organs from WT (Rab27$^{+/+}$), Rab27 Het (Rab27$^{+/-}$), and Rab27 KO (Rab27$^{-/-}$) mice; *n* = 6 mice/group. (B, left) Representative flow cytometry of CD11a antibody (Ab) staining (surface) and mYFP intensities (total) of naive CD11a-mYFP (WT) and CD11a-mYFP/Rab27 KO (Rab27$^{-/-}$) CD8⁺ T cells. (B, right) Graph shows quantification of surface versus intracellular CD11a antibody staining of naive CD8⁺ T cells from WT (Rab27$^{+/+}$) and Rab27 KO (Rab27$^{-/-}$) mice; *n* = 3 mice. (C) Representative flow cytometry of surface and intracellular (total) CD11a antibody staining of naive Rab27 KO CD8⁺ T cells; *n* = 3 mice. (D) Migration of naive CD8⁺ T cells from WT and Rab27 KO mice on ICAM-1+CCL21–coated surface; *n* = 3 mice (75–165 cells per mouse). Data are expressed as mean ± SEM. (E and F) Conjugation rates (E; *n* = 3 mice/group, 75–195 cells/mouse, PBS; percentage of conjugations with PBS-treated APCs) and contact duration (F; circles represent individual cells from three independent experiments with mean shown as a line) from real-time imaging of CD8⁺ T cells from OT-I and Rab27 KO/OT-I mice with N4-bearing APCs. Data represent mean ± SEM. (G) Representative Western blot of phosphorylated CD3ζ (pCD3ζ) expression in naive CD8⁺ T cells from WT and Rab27 KO mice after CD3/CD28 stimulation for indicated times; *n* = 2. (H) Representative flow cytometry of activation markers of WT versus Rab27 KO mice on indicated days after in vitro activation; *n* = 3 mice. (I) Ratio of naive WT and Rab27 KO CD8⁺ T cells in pooled lymph nodes 24 hpi; *n* = 3 mice.

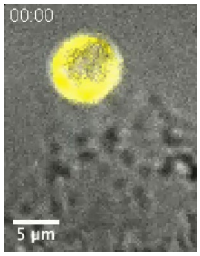

Video 1. **Localization of LFA-1 in naive CD8+ T cells.** Representative real-time imaging of naive CD8+ T cell contact with APCs loaded with N4 peptide on plates coated with ICAM-1 and CCL21.

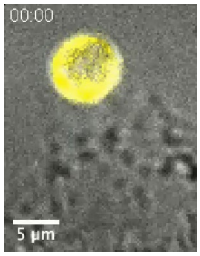

Video 2. **Localization of LFA-1 during naive CD8+ T cell migration.** Representative real-time imaging of a naive CD8+ T cell migrating on plates coated with ICAM-1 and CCL21.

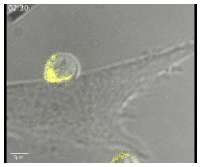

Video 3. **Intracellular LFA-1 redistribution to the contact site with antigen-bearing APCs.** Representative real-time imaging of naive CD8+ T cell contact with APCs loaded with N4 peptide on plates coated with ICAM-1 and CCL21.

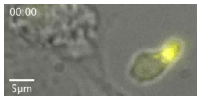

Video 4. **Intracellular LFA-1 fails to redistribute to the contact site upon encountering APCs bearing altered peptide ligands with reduced TCR affinity.** Representative real-time imaging of naive CD8+ T cell contact with APCs loaded with D7 peptide on plates coated with ICAM-1 and CCL21.

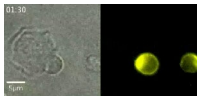

Video 5. **A CD8+ T cell asymmetrically divides in real time.** CD11a-mYFP CD8+ T cell division on ICAM-1–coated plates during contact with antigen-bearing APCs results in unequal partitioning of LFA-1 (CD11a-mYFP) into proximal (P) and distal (D) daughter cells.